

# Crystallization of a designed peptide from a molten globule ensemble

Stephen F Betz<sup>1</sup>, Daniel P Raleigh<sup>1†</sup>, William F DeGrado<sup>1</sup>, Brett Lovejoy<sup>2‡</sup>, Daniel Anderson<sup>2</sup>, Nancy Ogihara<sup>2</sup> and David Eisenberg<sup>2</sup>

**Background:** The design of amino acid sequences that adopt a desired three-dimensional fold has been of keen interest over the past decade. However, the design of proteins that adopt unique conformations is still a considerable problem. Until very recently, all of the designed proteins that have been extensively characterized possess the hallmarks of the molten globular state. Molten globular intermediates have been observed in both equilibrium and kinetic protein folding/stability studies, and understanding the forces that determine compact non-native states is critical for a comprehensive understanding of proteins. This paper describes the solution and early solid state characterization of peptides that form molten globular ensembles.

**Results & Conclusions:** Crystals diffracting to 3.5 Å resolution have been grown of a 16-residue peptide ( $\alpha_1A$ ) designed to form a tetramer of  $\alpha$ -helices. In addition, a closely related peptide,  $\alpha_1$ , has previously been shown to yield crystals that diffract to 1.2 Å resolution. The solution properties of these two peptides were examined to determine whether their well defined crystalline conformations were retained in solution. On the basis of an examination of their NMR spectra, sedimentation equilibria, thermal unfolding, and ANS binding, it is concluded that the peptides form  $\alpha$ -helical aggregates with properties similar to those of the molten globule state. Thus, for these peptides, the process of crystallization bears many similarities to models of protein folding. Upon dissolution, the peptides rapidly assume compact molten globular states similar to the molten globule like intermediates that are formed at short times after refolding is initiated. Following a rate-determining nucleation step, the peptides crystallize into a single or a small number of conformations in a process that mimics the formation of native structure in proteins.

## Introduction

The effective design of amino acid sequences that adopt a desired three-dimensional fold has progressed over the past decade [1,2]. Whereas the majority of early design efforts focused on  $\alpha$ -helical bundles [3,4], recent designs have focused on  $\beta$ -sheet proteins [5,6] and mixed  $\alpha$ - $\beta$  proteins [7–10]. Yet these proteins, and most other designed proteins that have been well characterized in solution, possess some of the properties of the ‘molten globular’ state [11]. Used here, the term ‘molten globule’ refers to a compact state that possesses a high degree of secondary structure, but a more dynamic hydrophobic interior [12–15]. On the other hand, the design of peptides that mimic various aspects of protein structure has been more successful [16–20]. Peptides that adopt  $\beta$ -turns [16], monomeric helices [19], and helix-turn-helix hairpins [21,22] have been designed and their structures determined by NMR and X-ray crystallography. In addition, a helix-turn-helix peptide that self-assembles into a native-like four-helix structure has been reported [23,24],

as has the self-assembly of a heterotrimeric  $\alpha$ -helical complex [25].

The work described in this paper continues the thread of peptide and protein design that has focused on the design, construction, and crystallographic characterization of  $\alpha$ -helical peptides that self-assemble into protein-like structures [26,27]. One class of peptides that has been extensively characterized [28–30] is a family of 12–16-residue amphiphilic  $\alpha$ -helices, the prototype of which is  $\alpha_1A$  (see Fig. 1). This 16-residue peptide contains leucine residues arranged along one face of the helix to form stabilizing helix-helix hydrophobic interactions. The opposite face of the helix consists of glutamine and lysine residues that electrostatically stabilize the structure and provide aqueous solubility. During the synthesis of  $\alpha_1A$ , a 12-residue fragment of the desired sequence was isolated (designated  $\alpha_1$ ), and its crystal structure determined at low pH [26]. As in the design, the structure consists of a hydrophobically stabilized cluster of  $\alpha$ -helices. However,

Addresses: <sup>1</sup>Chemical and Physical Sciences Department, The DuPont Merck Pharmaceutical Company, PO Box 80328, Wilmington DE 19880-0328, USA. <sup>2</sup>Molecular Biology Institute and Department of Chemistry and Biochemistry, UCLA, Los Angeles CA 90024-1570, USA. <sup>†</sup>Present address: Department of Chemistry, SUNY Stony Brook, Stony Brook NY 11794, USA. <sup>‡</sup>Present address: Glaxo Wellcome, 5 Moore Drive, Research Triangle Park, NC 27709, USA.

Correspondence to: William F DeGrado  
E-mail address:  
degradwf@lldmpc.dnet.dupont.com

Key words: crystallization, molten globule, protein design, protein folding

Received: 17 Nov 1995  
Revisions requested: 08 Dec 1995  
Revisions received: 18 Dec 1995  
Accepted: 20 Dec 1995

Published: 18 Jan 1996  
Electronic identifier: 1359-0278-001-00057

**Folding & Design** 18 Jan 1996, 1:57–64

© Current Biology Ltd ISSN 1359-0278

Figure 1

Peptide	Sequence
$\alpha_1$	Ac-ELLKKLLEELKG-OH
$\alpha_1A$	Ac-GKLEELLKKLLEELKG-OH
$\alpha_1B$	Ac-GELEELLKCLKELLKG-NH <sub>2</sub>

Nomenclature and primary sequences for the  $\alpha_1$  family of peptides.

the primary association in the crystal was a hexameric molecule. This unusual arrangement of helices may have been favored by the short length of the  $\alpha_1$  peptide as well as the low pH at which the peptide was crystallized. At neutral pH, the peptide crystallizes into an entirely different helical assembly featuring a tetramer in the asymmetric unit [31]. This finding prompted us to question whether the distinct structures of the peptide arose from different but stable aggregation states at low pH versus neutral pH, or whether it was a dynamic ensemble in solution.

We have also renewed our efforts to characterize the full-length  $\alpha_1A$  peptide, both in aqueous solution and in the solid state. We find that although this peptide shows the hallmarks of a molten globule in solution, it nevertheless yields diffraction-quality crystals. It was unexpected that  $\alpha_1A$  would form high-quality crystals because a closely

related peptide,  $\alpha_1B$ , had previously been shown to form molten globule like tetramers in solution [30], and crystallization efforts with  $\alpha_1B$  have thus far been unsuccessful. Investigation of the solution properties of  $\alpha_1A$  allows us to determine whether this peptide is more ordered than  $\alpha_1B$ , or whether diffraction-quality crystals had indeed grown from a molten globule ensemble of conformational states.

## Results

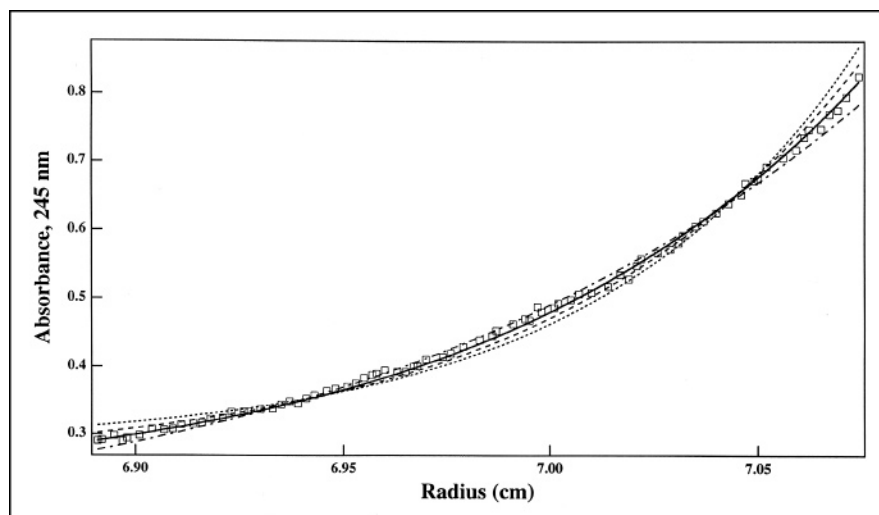
### Crystallization and solid state association

The  $\alpha_1A$  peptide was crystallized at neutral pH and ambient temperature yielding trigonal crystalline rods. If there is a peptide dimer in the asymmetric unit and a space group of P321 (see Materials and methods), a four- $\alpha$ -helical bundle is formed at the interface of two neighboring asymmetric units. The crystals of  $\alpha_1A$  are like those of globular proteins, although they appear less well ordered as indicated by their high mosaic spread (1.2°).

### Solution state association

The partial specific volumes and the solution oligomerization states of the  $\alpha_1$  and  $\alpha_1A$  peptides were determined under neutral conditions as described in Materials and methods. The initial concentration of peptide in the sedimentation equilibria experiments was approximately 2 mM where both peptides are fully associated [28]. At neutral pH,  $\alpha_1A$  was best fit as a single species to a molecular mass of 7242–7762 Da, corresponding to an aggregation state of 3.9–4.1 (Fig. 2), consistent with earlier data showing that  $\alpha_1A$  assumed a highly cooperative monomer/tetramer equilibrium [28]. No intermediate states could be discerned, although the small molecular mass of the monomer (1883 Da) coupled to our limitation in highest available rotor speed (48000 rpm) and the relatively high initial peptide concentration made accurate

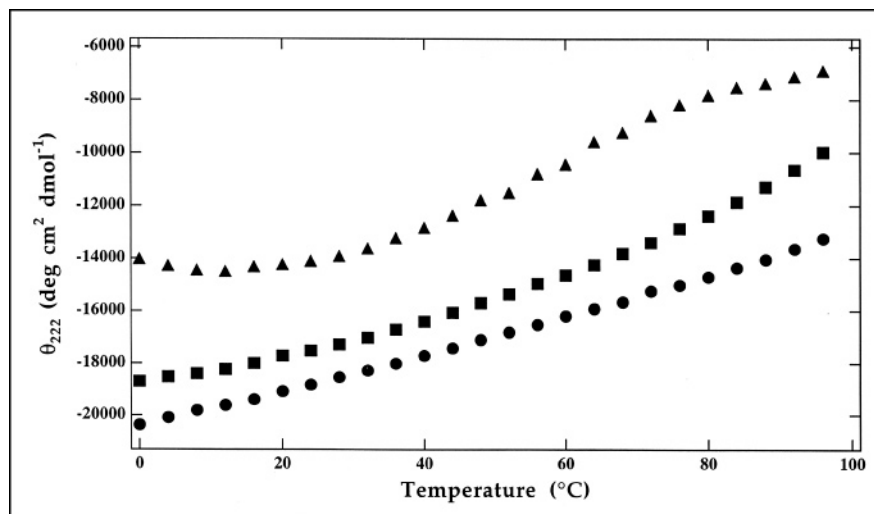
Figure 2



Sedimentation equilibrium of  $\alpha_1A$ . Absorbance at 245 nm versus radius for raw data (squares) and different theoretical monomer/*n*mer fits for 2 mM  $\alpha_1A$  in 50 mM MOPS pH 7.0, 298 K, at 48 000 rpm. Dot-dashed line, fit to trimer; Solid line, fit to tetramer; Dashed line, fit to pentamer; Dotted line, fit to hexamer.

Figure 3

Mean residue ellipticity at 222 nm versus temperature for  $\alpha_1A$  in 50 mM MOPS, pH 6.6. Sample concentrations were 2 mM (circles), 200  $\mu$ M (squares), and 20  $\mu$ M (triangles).



determination of  $K_d$  difficult. Under these conditions, the concentration of the associated species far exceeds that of the monomer (the midpoint of the association equilibrium is approximately 35  $\mu$ M). Nevertheless, the determined value ( $K_d \sim 10^{-13} M^3$ ) is in reasonable agreement with the value of  $2 \times 10^{-14} M^3$  determined by Ho and DeGrado [28] under slightly different conditions. Thus, at accessible experimental conditions,  $\alpha_1A$  is almost fully tetrameric.

In contrast to the well defined aggregation behavior observed for  $\alpha_1A$ , the predominant aggregation state of the shorter  $\alpha_1$  peptide depended on the concentration of the peptide. The sedimentation data were fitted to cooperative monomer/ $n$ -mer aggregation schemes. At an initial loading concentration of 400  $\mu$ M, the sedimentation data were best described by a monomer/pentamer equilibrium, in reasonable agreement with earlier concentration-dependent circular dichroism (CD) experiments under comparable conditions, which showed a cooperativity of four. As the concentration is further increased, however, higher order aggregates are formed. At an initial loading concentration of 2 mM, the data are best fit to an aggregation state of 8.0. The CD and sedimentation equilibrium data together suggests a complex association, with the minimal stable association state of  $\alpha_1$  approximately four. However, this aggregate can non-cooperatively associate further to form higher order aggregates. This second process was not apparent in earlier CD experiments [17] presumably because it does not involve a change in secondary structure content. The formation of higher aggregates was readily apparent in the sedimentation studies, though, because the buoyant molecular weight changes as the aggregation state changes. These results illustrate the complementarity of these two methods for measuring both the minimal

stable association state and the actual association at a given concentration.

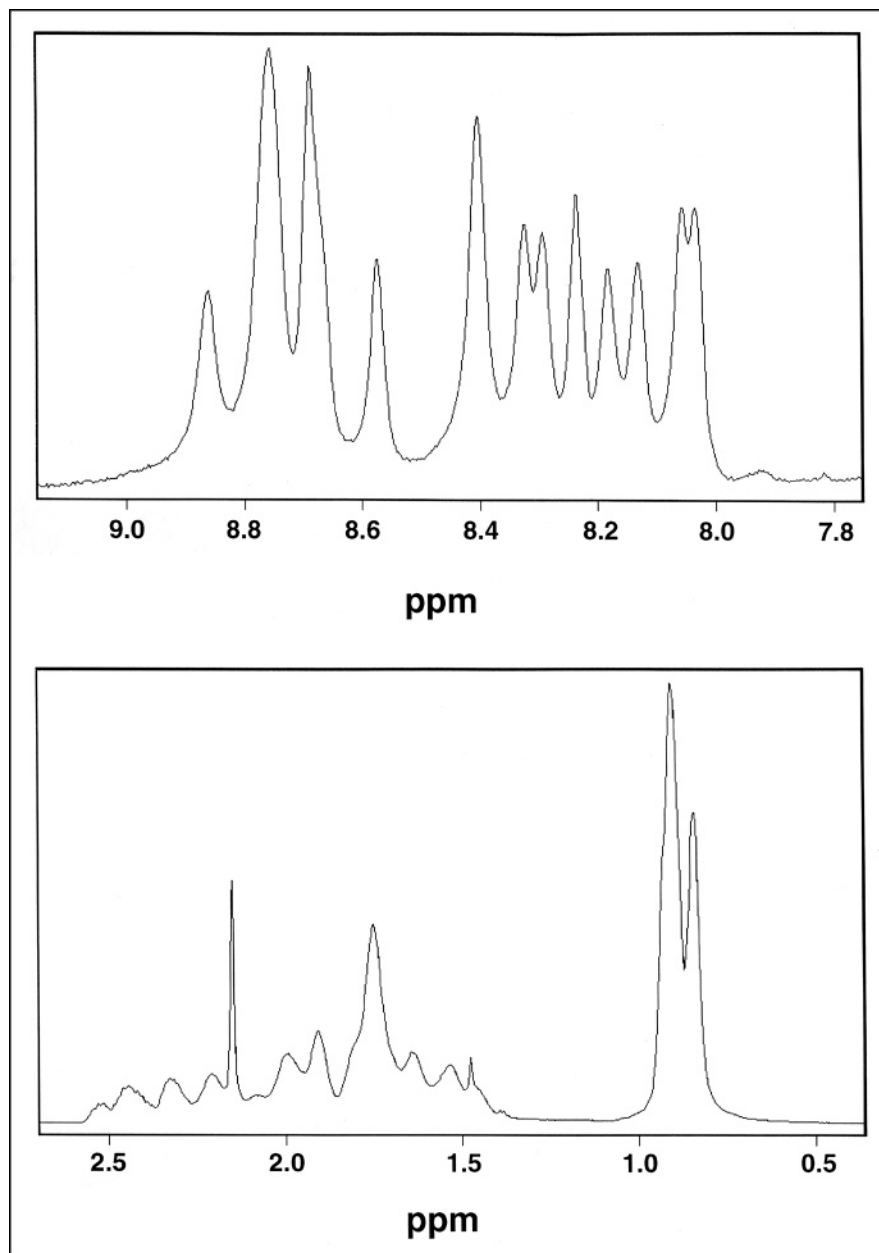
#### Circular dichroism

The concentration-dependent thermal denaturation of  $\alpha_1A$  monitored at 222 nm is shown in Figure 3. At high concentrations, non-cooperative gradual unfolding is observed with increasing temperature. To determine whether this behavior is a consequence of an extremely stable tetramer, or simply low values of  $\Delta H$  and  $\Delta C_p$ , the experiment was also carried out near the midpoint of the concentration-dependent transition where temperature-dependent changes in association should be readily observed. At 20  $\mu$ M, broad sigmoidal denaturation curves are observed, indicating that the unfolding occurs with low values of  $\Delta H$  and  $\Delta C_p$ , as is frequently observed for molten globules [15,32,33]. In short, thermal denaturation of  $\alpha_1A$  suggests that the tetramer behaves more like previously characterized molten globules than native-like proteins.

#### NMR solution behavior

The one-dimensional NMR spectra of  $\alpha_1A$  at 20°C and pH 5.5 is shown in Figure 4. The amide proton region is reasonably well dispersed and two-dimensional NOESY spectra show a series of  $NH_i$  to  $NH_{i+1}$  crosspeaks (DP Raleigh, unpublished data). Both these observations are consistent with a well defined  $\alpha$ -helical conformation. Similar observations have been made for the  $\alpha_1$  [29] and  $\alpha_1B$  peptides [30]. The methyl resonances are poorly defined at both pH values. This lack of dispersion is partly due to the absence of aromatic moieties, but it also suggests that there is rapid averaging of the core on the NMR time scale. Therefore, the secondary structure of  $\alpha_1A$  appears well defined, whereas the conformations of the interior sidechains are not.

Figure 4



One-dimensional <sup>1</sup>H NMR spectra for  $\alpha_1A$  in water at 20°C, pH 5.5. (a) Amide region. (b) Aliphatic region. Sample concentration was 4 mM.

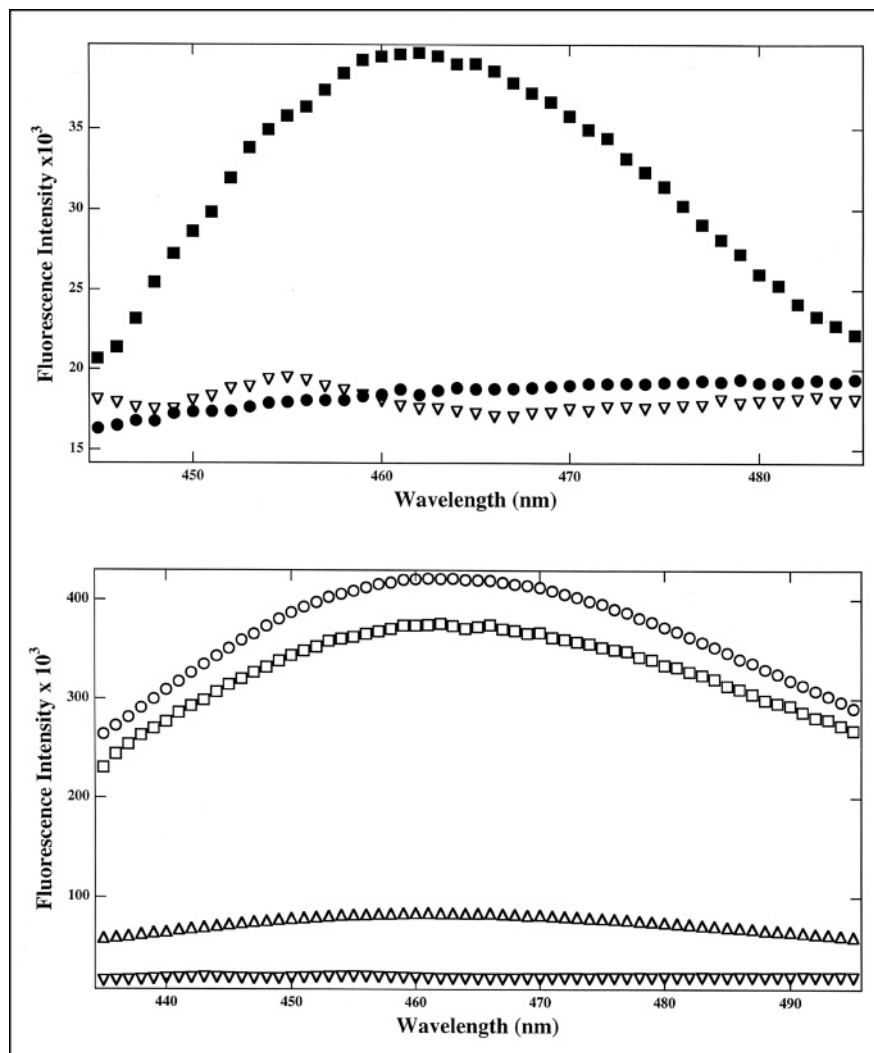
#### ANS-binding studies

The binding of 8-anilino-1-naphthalenesulfonic acid (ANS) to  $\alpha_1A$  was investigated. ANS is a hydrophobic dye that exhibits a large increase in fluorescence intensity when in an apolar environment. Experimental evidence correlates the binding of this dye with molten globular behavior [12–14,34]. The emission spectrum of ANS in the presence of  $\alpha_1A$  depends markedly on the concentration of the peptide (see Fig. 5a). At concentrations below the midpoint of association of the peptide, little binding is observed, but at higher concentrations a large change in intensity and emission maximum is observed. At peptide

concentrations at which most of the ANS is bound, the emission maximum of ANS bound to  $\alpha_1A$  is 462 nm, compared to 454–472 nm for ANS bound to protein molten globules under similar conditions [14]. Similar results were observed for the  $\alpha_1$  peptide. At low concentrations, no change in the fluorescence spectrum was observed, but at concentrations at which the peptide was aggregated an increase in quantum yield and a blue shift of the emission maximum were observed. At neutral pH, the emission maximum was shifted to 466 nm. Near pH 3, the quantum yield was further increased and the emission maximum shifted to 461 nm (see Fig. 5b). Thus, ANS-

Figure 5

ANS-binding of  $\alpha_1$  and  $\alpha_1A$ . (a) Fluorescence emission spectra of ANS alone (open, inverted triangles), and in the presence of 10  $\mu$ M  $\alpha_1A$  (closed circles), and 60  $\mu$ M  $\alpha_1A$  (closed squares) in 20 mM MES pH 6.5. (b) Fluorescence emission spectra of ANS alone (open, inverted triangles), and in the presence of 2 mM  $\alpha_1A$  in 20 mM MES pH 6.2 (open circles), and 2 mM  $\alpha_1$  in 20 mM MES pH 6.5 (open triangles), and 2 mM  $\alpha_1$  in 20 mM NaOAc pH 3.3 (open squares).



binding suggests a molten globule like character for both  $\alpha_1$  and  $\alpha_1A$ .

## Discussion

### The solution characteristics of $\alpha_1$ and $\alpha_1A$

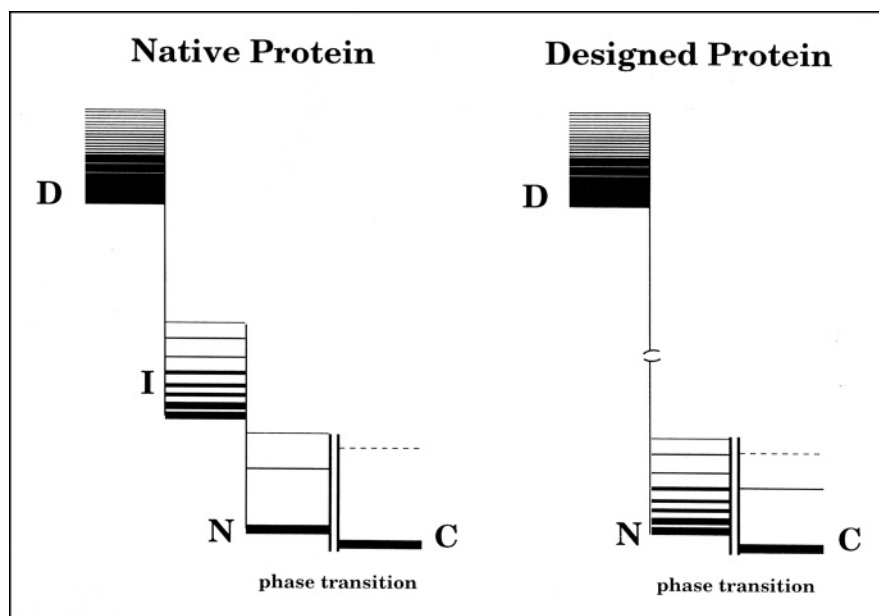
Extensive solution measurements of  $\alpha_1$  have previously shown [17,29] that this peptide associates into oligomers in which the monomers assume well ordered,  $\alpha$ -helical backbone conformations. However, these aggregates are not as well ordered as in native proteins. A variety of association states are observed, depending on the peptide concentration, and the monomers are in rapid equilibrium with the associated form on the millisecond time scale [29], indicating that there is a small activation energy for the association/dissociation of these peptides. There is very little dispersion of the sidechain resonances of this peptide, and it also binds ANS. Both of these features suggest that the oligomers have poorly ordered interior sidechains.

The properties of  $\alpha_1A$  parallel those of  $\alpha_1$  in many regards. The lack of dispersion in the sidechain region of the NMR spectrum, the binding of ANS, and the lack of a well defined thermal unfolding transition collectively provide strong evidence for a molten globule like ensemble. One difference, however, is that  $\alpha_1A$  very cooperatively assembles into a single, tetrameric aggregation state. Yet, despite its dynamic properties,  $\alpha_1A$  is able to form diffraction quality crystals; similarly,  $\alpha_1$  crystallizes in an extremely well ordered state capable of diffraction of X-rays beyond 1  $\text{\AA}$ .

### Crystallization as a mimic of protein folding

The fact that  $\alpha_1$  and  $\alpha_1A$  form diffraction-quality crystals suggests that they are capable of assuming particular conformations that are stable enough to nucleate crystallization. Thus, the process of crystallization of these peptides bears many similarities to models of protein

Figure 6



Hypothetical energy relationship for the folding and crystallization of a natural protein and designed proteins like  $\alpha_1$  and  $\alpha_1A$ . The bars symbolize the number of energy states populated in each regime. The highest bar (or dashed bar) represents the upper limit of  $kT$ . The denatured state (D) is represented by a large number of conformations. Whereas a natural protein has a well defined native state (N) in solution, the designed protein exists as an ensemble with many nearly equivalent energetic states, similar to proposed intermediates (I) in the folding of naturally occurring proteins. In the crystalline state (C), both have defined structures, although for the case of  $\alpha_1A$ , the limited resolution and high mosaic spread of its crystals suggest that they are composed of more substates than the most well ordered protein crystals.

folding that involve molten globule like intermediates: upon dissolution in water, the peptide rapidly assumes a compact globular structure consisting of an ensemble of interconverting conformational states. Following nucleation, the peptide crystallizes in a single (or small number of) conformation(s). Proteins are often hypothesized to adopt their unique, folded conformations by mechanisms that involve formation of molten globular intermediates [35]. The essential difference between these designed proteins and naturally occurring ones is that a natural protein contains sufficient information in its sequence to specify a unique conformation, whereas crystal packing forces are necessary to order the conformations of  $\alpha_1$  and  $\alpha_1A$  (Fig. 6). The two designed proteins described here differ in that  $\alpha_1A$  is able to form a meta-stable structure in solution, whereas  $\alpha_1$  indiscriminately associates with increasing concentration. Crystal packing forces seem nearly totally responsible for the structure of  $\alpha_1$  (i.e. the energy difference between the native solution ensemble [N] and crystalline [C] states is large), but appear less so, and more akin to the final stages of protein folding, in the formation of the  $\alpha_1A$  structure.

A final conclusion of this study is that because of their dynamic properties, designed peptides and proteins may have different structural characteristics in solution and in the solid state. Thus, it is more important with designed proteins than natural proteins to examine thoroughly the solution properties prior to concluding that the crystallographically determined structure represents the full conformational properties in solution.

## Materials and methods

### Peptide synthesis and purification

The peptide was synthesized by standard automated methods on a Milligen 9050 and purified by reverse phase HPLC. Specifically, using a loading volume of 1 ml of 10 mg ml<sup>-1</sup> crude peptide, pure  $\alpha_1A$  was collected after 16.5 min during a 20-min gradient from 10–75% CH<sub>3</sub>CN in the presence of 0.05% TFA on a 25 mm × 200 mm Radial-Pak preparative  $\mu$ Bondpak C18 column (Waters) with a flow rate of 15.7 ml min<sup>-1</sup>.

### Crystallization conditions

Crystals of  $\alpha_1A$  were grown by the sitting drop method. Drops were prepared by mixing 12  $\mu$ l of a 20 mg ml<sup>-1</sup> solution and 12  $\mu$ l of a reservoir solution that consisted of a 25 mM imidazole buffer adjusted to pH 7.0 with HCl, 23% (w/v) polyethylene glycol-8000 and 14.3% (v/v) ethanol. Crystalline rods measuring 1.0 × 0.2 × 0.1 mm grew within 11 d of incubation at 22°C. Crystallization at 4°C and 30°C had no significant effect on crystal size.

### Space group determination

To determine the space group of  $\alpha_1A$ , data to 5 Å resolution were collected on a single crystal using an AFC5R diffractometer (Rigaku). Data reduction using MSC software (Molecular Structure Corporation) indicated that the crystals belonged either to the trigonal/rhombohedral or hexagonal crystal systems. The cell parameters are  $a = b = 51.0$  Å,  $c = 23.9$  Å,  $\alpha = \beta = 90^\circ$  and  $\gamma = 120^\circ$ . Further analysis of the data set revealed that one rule for six-fold symmetry  $[F(hk\ell)] = [F(hk\ell)]$  is not obeyed, thus eliminating all hexagonal space groups. The rhombohedral space groups  $R_3$  and  $R_{32}$  were also ruled out by the presence of  $-h + k + \ell \neq 3n$  reflections (hexagonal indexing). Analysis of the data also revealed the presence of a two-fold axis half-way between  $a^*$  and  $b^*$ , thus limiting the possible space groups to  $P3_121$  (where  $x$  is 0, 1, or 2). The finding that reflections  $l \neq 3n$  along the 00 $l$  line were present in the data indicated that the space group is  $P321$ . Based on this space group and a molecular mass of 1883 Da per monomer, there is either a peptide trimer or peptide dimer in the asymmetric unit (corresponding respectively to  $V_m = 1.59$  or 2.38 Å<sup>3</sup> Da<sup>-1</sup>) ADDIN [36]. A peptide monomer in the asymmetric unit

is highly unlikely because the corresponding Matthews number,  $V_m = 4.77 \text{ \AA}^3 \text{ Da}^{-1}$ , exceeds the 1.68–3.53  $\text{Å}^3 \text{ Da}^{-1}$  range that is typically observed for protein crystals [36].

#### Analytical ultracentrifugation

Sedimentation equilibrium analysis was performed with a Beckman XLA analytical ultracentrifuge. Initial peptide concentrations were 2–4 mg ml<sup>-1</sup> in 50 mM MOPS, pH 7.0 or 50 mM NaOAc, pH 3.3. High concentrations were chosen so that the peptides would be nearly fully associated in solution. The samples were centrifuged at 35 000, 42 000, and 48 000 rpm. Equilibrium was determined when successive radial scans at the same speed were indistinguishable.

The behavior of a single species at equilibrium can be described by the following equation:

$$M_b = M_w (1 - \bar{v}\rho) \quad (1)$$

in which  $M_b$  is the measured buoyant molecular mass,  $M_w$  is the molecular mass in Daltons,  $\bar{v}$  is the partial specific volume of the protein, and  $\rho$  is the density of the sample solution. Accurate determination requires that both the density and partial specific volume be known. The densities of the solutions were measured with an Anton–Paar DMA–602 external measuring cell using a sampling frequency of 2 kHz. Determinations were made under the same conditions as the sedimentation experiments. The aggregation state was determined by fitting the data to either a single monomeric species or by monomer/mer equilibria, using the software package Igor Pro (WaveMetrics). Radial absorbance spectra were recorded at several appropriate wavelengths and were shown to yield indistinguishable results.

The determination of association of a species also requires that the partial specific volume,  $\bar{v}$ , be accurately known. Using a method based on residue composition [37,38], the calculated  $\bar{v}$  for  $\alpha_1A$  is 0.78 ml g<sup>-1</sup>, and the calculated  $\bar{v}$  for  $\alpha_1$  is 0.80 ml g<sup>-1</sup>. These values are somewhat higher than those measured for typical globular proteins, 0.70–0.75 ml g<sup>-1</sup> [39]. As a result of their minimalist design, their associative character, and their atypical amino acid composition compared with naturally occurring proteins, the values of  $\bar{v}$  calculated by residue composition alone may not reflect their true values when associated in solution. The partial specific volumes of  $\alpha_1$  and  $\alpha_1A$  were measured experimentally from simultaneous determination of its buoyant molecular mass in H<sub>2</sub>O and D<sub>2</sub>O-based buffer systems [40]. The partial specific volume of  $\alpha_1A$  determined by this method was 0.75 ml g<sup>-1</sup>, and that of  $\alpha_1$  was determined to be 0.77 ml g<sup>-1</sup>. As a control, the partial specific volume of horseheart cytochrome *c* (Sigma) was determined to be 0.72 ml g<sup>-1</sup> by the same method, in close agreement with the value of 0.725 ml g<sup>-1</sup> reported by Gekko & Hasegawa [39].

#### NMR spectroscopy

<sup>1</sup>H NMR spectra were recorded with a Bruker AMX-600 spectrometer at 20°C using presaturation of the water resonance. One-dimensional spectra were recorded with 8K points. The raw data were transformed and phased using Felix 2.2 software (Hare/Biosym).

#### Fluorescence measurements

Fluorescence of ANS–peptide complexes were performed on a Spex Fluorolog fluorimeter at 25°C. The formation of ANS peptide complexes was monitored by titrating peptide into a constant amount (5  $\mu\text{M}$ ) of ANS in a 1 cm cuvette. Buffer conditions were 20 mM MES, pH 6.5. The excitation wavelength was 370 nm with emission spectra recorded from 420–500 nm.

#### Circular dichroism

The circular dichroism of peptide solutions was monitored with an AVIV 62 DS spectropolarimeter interfaced to an IBM PC. Buffer conditions were 50 mM MOPS, pH 6.6, or 50 mM sodium acetate, pH 3.3. The

concentration of peptide for the CD experiments ranged from 20  $\mu\text{M}$  to 1 mM. Mean residue ellipticities ( $^\circ \text{ cm}^2 \text{ dmol}^{-1}$ ) were calculated using the equation:

$$[\theta_{222}] = (\theta_{\text{obsd}}/10l)/n \quad (2)$$

in which  $\theta_{\text{obsd}}$  is the ellipticity measured in millidegrees,  $l$  is the length of the cell in cm,  $c$  is the peptide concentration in mol l<sup>-1</sup>, and  $n$  is the number of residues.

## Acknowledgements

We thank Jim Lear for assistance with the sedimentation equilibrium experiments, and Jim Bryson and Helen Lu for helpful discussions. Support for the crystallographic and design work was provided by NIH and NSF.

## References

- DeGrado, W.F., Wasserman, Z.R. & Lear, J.D. (1989). Protein design, a minimalist approach. *Science* **243**, 622–628.
- Bryson, J.W., Betz, S.F., Lu, H.S., Suich, D.J., Zhou, H.X., O'Neil, K.T. & DeGrado, W.F. (1995). Protein design, a hierarchic approach. *Science* **270**, 935–941.
- Regan, L. & DeGrado, W.F. (1988). Characterization of a helical protein designed from first principles. *Science* **241**, 976–978.
- Hecht, M.H., Richardson, J.S., Richardson, D.C. & Ogden, R.C. (1990). *De novo* design, expression and characterization of felix: a four-helix bundle protein of native-like sequence. *Science* **249**, 884–891.
- Yan, Y. & Erickson, B.W. (1994). Engineering of betabellin 14D: disulfide-induced folding of a  $\beta$ -sheet protein. *Protein Sci.* **3**, 1069–1073.
- Quinn, T.P., Tweedy, N.B., Williams, R.W., Richardson, J.S. & Richardson, D.C. (1994). Betadoublet: *de novo* design, synthesis, and characterization of a  $\beta$ -sandwich protein. *Proc. Natl. Acad. Sci. U.S.A.* **91**, 8747–8751.
- Goraj, K., Renard, A. & Martial, J.A. (1990). Synthesis, purification and initial structure characterization of octarellin, a *de novo* polypeptide modelled on the alpha/beta barrel proteins. *Protein Eng.* **3**, 259–266.
- Fedorov, A.N., *et al.*, & Ptitsyn, O.B. (1992). *De novo* design, synthesis, and study of Albebetin, a polypeptide with a predetermined three-dimensional structure. *J. Mol. Biol.* **225**, 927–931.
- Tanaka, T., Kimura, H., Hayashi, M., Fujiyoshi, Y., Fukuhara, K.-I. & Nakamura, H. (1994). Characteristics of a *de novo* designed protein. *Protein Sci.* **3**, 419–427.
- Houbrechts, A., *et al.*, & Goraj, K. (1995). Second generation octarellins: two new *de novo* ( $\beta/\alpha$ )<sub>8</sub> polypeptides designed for investigating the influence of  $\beta$ -residue packing on the  $\alpha/\beta$  barrel structure stability. *Protein Eng.* **8**, 249–259.
- Betz, S.F., Raleigh, D.P. & DeGrado, W.F. (1993). *De novo* protein design: from molten globules to native-like states. *Curr. Opin. Struct. Biol.* **3**, 601–610.
- Kuwajima, K. (1989). The molten globule state as a clue for understanding the folding and cooperativity of globular-protein structure. *Proteins* **6**, 87–103.
- Ptitsyn, O.B. (1992). The molten globule state. In *Protein Folding*. (Crieghton, T.E., ed.), pp. 243–299, Freeman, New York.
- Semisotnov, G.V., Rodionova, N.A., Razgulyaev, O.I., Uversky, V.N., Gripas, A.F. & Gilmanshin, R.I. (1991). Study of the "molten globule" intermediate state in protein folding by a hydrophobic fluorescent probe. *Biopolymers* **31**, 119–128.
- Haynie, D.T. & Friere, E. (1993). Structural energetics of the molten globule state. *Proteins* **16**, 115–140.
- Rose, G.D., Gierasch, L.M. & Smith, J.A. (1985). Turns in peptides and proteins. *Adv. Protein Chem.* **37**, 1–109.
- Eisenberg, D., Wilcox, W., Eshita, S.M., Pryciak, P.M., Ho, S.P. & DeGrado, W.F. (1986). The design, synthesis, and crystallization of an alpha-helical peptide. *Proteins* **1**, 16–22.
- DeGrado, W.F. (1988). Design of peptides and proteins. *Adv. Protein Chem.* **39**, 51–124.
- Chakrabarty, A., Kortemme, T. & Baldwin, R.L. (1994). Helix propensities of the amino acids measured in alanine-based peptides without helix-stabilizing side-chain interactions. *Protein Sci.* **3**, 843–852.
- O'Shea, E.K., Lumb, K.J. & Kim, P.S. (1993). Peptide 'Velcro': design of a heterodimeric coiled coil. *Curr. Biol.* **3**, 658–667.

21. Kuroda, Y., Nakai, T. & Ohkubo, T. (1994). Solution structure of a *de novo* helical protein by 2D-NMR spectroscopy. *J. Mol. Biol.* **236**, 862–868.
22. Fezoui, Y., Weaver, D.L. & Osterhout, J.J. (1994). *De novo* design and structural characterization of an  $\alpha$ -helical hairpin peptide: a model system for the study of protein folding intermediates. *Proc. Natl. Acad. Sci. U.S.A.* **91**, 3675–3679.
23. Raleigh, D.P. & DeGrado, W.F. (1992). A *de novo* designed protein shows a thermally induced transition from a native to a molten globule-like state. *J. Am. Chem. Soc.* **114**, 10079–10081.
24. Raleigh, D.P., Betz, S.F. & DeGrado, W.F. (1995). A *de novo* designed protein mimics the native state of natural proteins. *J. Am. Chem. Soc.* **117**, 7558–7559.
25. Nautiyal, S., Woolfson, D.N., King, D.S. & Alber, T. (1995). A designed heterotrimeric coiled coil. *Biochemistry* **34**, 11645–11651.
26. Hill, C.P., Anderson, D.H., Wesson, L., DeGrado, W.F. & Eisenberg, D. (1990). Crystal structure of  $\alpha_1$ : implications for protein design. *Science* **249**, 543–546.
27. Lovejoy, B., Choe, S., Cascio, D., McRorie, D.K., DeGrado, W.F. & Eisenberg, D. (1993). Crystal structure of a synthetic triple-stranded alpha-helical bundle. *Science* **259**, 1288–1293.
28. Ho, S.P. & DeGrado, W.F. (1987). Design of a 4-helix bundle protein: synthesis of peptides which self-associate into a helical protein. *J. Am. Chem. Soc.* **109**, 6751–6758.
29. Ciesla, D.J., Gilbert, D.E. & Feigon, J. (1991). Secondary structure of the designed peptide alpha-1 determined by nuclear magnetic resonance spectroscopy. *J. Am. Chem. Soc.* **113**, 3957–3961.
30. Osterhout, J.J., *et al.*, & DeGrado, W.F. (1992). Characterization of the structural properties of  $\alpha_1\beta$ , a peptide designed to form a four-helix bundle. *J. Am. Chem. Soc.* **114**, 331–337.
31. Prive, G., Ogihara, N., Wesson, L., Cascio, D. & Eisenberg, D. (1995). A designer peptide at high resolution: shake and bake solution of a 400 atom structure. *Am. Cryst. Assoc. Ann. Mtg.*
32. Ptitsyn, O.B. (1987). Protein folding hypotheses and experiments. *J. Protein Chem.* **6**, 273–293.
33. Griko, Y.V., Privalov, P.L., Venyaminov, S.Y. & Kutysenko, V.P. (1988). Thermodynamic study of the apomyoglobin structure. *J. Mol. Biol.* **202**, 127–138.
34. Ikeguchi, M., Kuwajima, K., Mitani, M. & Sugai, S. (1986). Evidence for identity between the equilibrium unfolding intermediate and a transient folding intermediate: a comparative study of the folding reaction of a-lactalbumin and lysozyme. *Biochemistry* **25**, 6965–6972.
35. Jennings, P.A. & Wright, P.E. (1993). Formation of a molten globule intermediate early in the kinetic pathway of apomyoglobin. *Science* **262**, 892–896.
36. Matthews, B.W. (1968). Solvent content of protein crystals. *J. Mol. Biol.* **33**, 491–497.
37. Cohn, E.J. & Edsall, J.T. (1943) Proteins, amino acids, and peptides as ions and dipolar ions. In *Proteins, Amino Acids, and Peptides as Ions and Dipolar Ions*, pp. 370–377, Reinhold Publishing Corp, New York.
38. Harding, S.E., Rowe, A.J. & Horton, J.C. (1992) *Analytical Ultracentrifugation in Biochemistry and Polymer Science*. The Royal Society of Chemistry, Cambridge.
39. Gekko, K. & Hasegawa, Y. (1986). Compressibility–structure relationship of globular proteins. *Biochemistry* **25**, 6563–6571.
40. Edelstein, S.J. & Schachman, H.K. (1973). Measurement of partial specific volume by sedimentation equilibrium in H<sub>2</sub>O–D<sub>2</sub>O solutions. *Methods Enzymol.* **27**, 82–98.